Acta Crystallographica Section D
Biological Crystallography
ISSN 0907-4449

SANS study of cellulose extracted from switchgrass

Sai Venkatesh Pingali,[a]* Volker S. Urban,[a] William T. Heller,[a] Joseph McGaughey,[b] Hugh M. O'Neill,[a] Marcus Foston,[c] Dean A. Myles,[a] Arthur J. Ragauskas[c] and Barbara R. Evans[b]

[a]Center for Structural Molecular Biology (CSMB), Oak Ridge National Laboratory, Oak Ridge, TN 37831, USA, [b]Molecular Biosciences and Biotechnology Group, Chemical Sciences Division, Oak Ridge National Laboratory, Oak Ridge, TN 37831, USA, and [c]Institute of Paper Science and Technology, School of Chemistry and Biochemistry and Georgia Institute of Technology, Atlanta, GA 30332, USA

Correspondence e-mail: pingalis@ornl.gov

Received 18 April 2010
Accepted 28 May 2010

Lignocellulosic biomass, which is an abundant renewable natural resource, has the potential to play a major role in the generation of renewable biofuels through its conversion to bioethanol. Unfortunately, it is a complex biological composite material that shows significant recalcitrance, making it a cost-ineffective feedstock for bioethanol production. Small-angle neutron scattering (SANS) was employed to probe the multi-scale structure of cellulosic materials. Cellulose was extracted from milled native switchgrass and from switchgrass that had undergone a dilute acid pretreatment method in order to disrupt the lignocellulose structure. The high-Q structural feature ($Q > 0.07$ Å^{-1}) can be assigned to cellulose fibrils based on a comparison of cellulose purified by solvent extraction of native and dilute acid pretreated switchgrass and a commercial preparation of microcrystalline cellulose. Dilute acid pretreatment results in an increase in the smallest structural size, a decrease in the interconnectivity of the fibrils and no change in the smooth domain boundaries at length scales larger than 1000 Å.

1. Introduction

Lignocellulosic biomass from terrestrial plants has the potential to supply a renewable feedstock for the production of ethanol and other transportation fuels (Lynd *et al.*, 1991; Himmel *et al.*, 2007). Of the many types of plants examined as potential feedstocks, the advantages of herbaceous crops, particularly grasses, include fast growth, established agricultural cultivation and the potential for dual-purpose production. The native North American prairie grass switchgrass (*Panicum virgatum*) possesses the additional advantages of perennial growth, production of seeds, high yields and adaptability to poor soils (Bouton, 2007, 2008).

Biomass is largely composed of cellulose, a linear polymer of β-1,4-linked glucose chains assembled into partially crystalline fibers, hemicellulose, a heterogeneous branched polymer of pentose and hexose sugars, and lignin, which is composed of extensively cross-linked methoxy-substituted phenylpropane units. Cellulose is the main structural component and can be enzymatically hydrolyzed to provide glucose for fermentative ethanol production. In lignocellulosic biomass, cellulose hydrolysis is impeded by hemicellulose and lignin layers and also by the fibrous crystalline structure of the cellulose itself (McMillan, 1994). Therefore, the efficient hydrolysis of lignocellulosic biomass requires mechanical and chemical deconstruction of the plant cell walls.

Effective pretreatments increase the gross material porosity, decrease the crystallinity of the cellulose fibrils, remove hemicellulose and reduce the lignin present (McMillan, 1994). Although the efficiency of cellulose hydrolysis is greatly increased by dilute acid pretreatment, it does not fully remove lignin, which is thought to precipitate on the cellulose surface and to inhibit the hydrolysis process through a combination of binding with the cellulase enzymes and blockage of the progress of the enzymes along the glucose chains (Lee *et al.*, 2000; Zhang & Lynd, 2004).

Here, we present a characterization of the multi-scale hierarchical structures of celluloses that have been extracted from untreated and dilute acid pretreated switchgrass and commercial microcrystalline cellulose. Traditionally, hierarchically structured materials require multiple techniques to probe the structure at the different length scales present, including optical microscopy, SEM, AFM and NMR for length scales ranging from millimetres to nanometres, yet many of these techniques provide highly localized information on the surface of the material. In this study, we used small-angle neutron scattering (SANS) to probe the impact of dilute acid treatment on the structure of bulk cellulose. SANS is a powerful tool for studying bulk materials that probes length scales ranging from 10 to 10 000 Å and is ideal for studying the morphology of complex materials over multiple length scales.

2. Materials and experimental methods

2.1. Switchgrass cellulose preparation

For the native sample, switchgrass was milled using a Wiley mill to pass through a 0.05 mm pore-size screen or 80–20 mesh screens and was used without further treatment. To extract cellulose, native switchgrass underwent further processing prior to extraction with 2:1(*v*:*v*) benzene:ethanol for 24 h in a Soxhlet apparatus to remove extractives. The solvent was removed and extractive-free switchgrass (1.5 g) was dispersed in 125 ml de-ionized water in a Kapak sealing pouch. The resulting mixture was heated in a water bath for 1 h at 348 K prior to the addition of 1 ml glacial acetic acid and 1 g sodium chlorite ($NaClO_2$) and continuation of the reaction for an additional 1 h. This procedure was repeated three times to give a total treatment time of 3 h. The treated sample was then quenched in ice–water, filtered and washed thoroughly using de-ionized water and acetone before the holocellulose isolated from the switchgrass was treated with 2.5 *M* hydrochloric acid at 373 K for 4 h. The treated sample was washed with de-ionized water and acetone and air-dried to remove hemicellulose and obtain cellulose (Foston *et al.*, 2009).

2.2. Dilute acid pretreatment switchgrass cellulose

A Wiley-milled switchgrass sample was presoaked at room temperature (298 K) while continuously stirring in ∼1% dilute sulfuric acid solution at 5%(*w*/*w*) dry solids for 4 h. The presoaked slurry was filtered and transferred into a 4560 mini-Parr 300 ml pressure reactor (Parr Instrument Company) in ∼1% (or 0.1–0.2 *M*) dilute sulfuric acid solution at 5%(*w*/*w*) solids and sealed. The impeller speed was set to ∼100 rev min^{-1} and the vessel was heated to 433 K over ∼30 min (at ∼6 K min^{-1}). The reactor was held at 433 ± 2 K (648–689 kPa) for 2 min (±0.5 min) residence time. To halt the pretreatment process, the reactor was quenched in an ice bath after cooling to 343 K (in ∼5 min). The pretreated slurry was then filtered to remove the solid residue and washed with an excess of de-ionized water and dried overnight at room temperature. The yields of biomass recovered after pretreatment ranged between 75 and 85% of the initial material by mass. Cellulose was isolated from the pretreated material by extraction of lignin using the extraction procedure described above in §2.1 to obtain holocellulose (Esteghlalian *et al.*, 1997; Schell *et al.*, 2003; Foston *et al.*, 2009).

2.3. Microcrystalline cellulose: Avicel

Microcrystalline cellulose (Avicel; PH-105) was purchased from FMC Corporation, USA and was used without further purification (Zhang *et al.*, 2006). The crystalline isomorph of this material is cellulose I and its average particle size is 20 µm. Avicel suspensions were prepared in D_2O for SANS scattering studies.

2.4. Small-angle neutron scattering (SANS)

SANS measurements were performed with the CG-3 Bio-SANS instrument (Lynn *et al.*, 2006) at the High Flux Isotope Reactor (HFIR) facility of Oak Ridge National Laboratory. All samples were soaked in 100% D_2O solvent using 2–3 times the volume of the solid sample for over 24 h to maximize D/H exchange and solvent penetration. The coarse-milled switchgrass samples immersed in D_2O were placed in 0.5 mm thick quartz cells with detachable cell walls (Hellma Model No. 106-QS 0.5 mm) for SANS studies. The switchgrass particles were densely packed and did not settle over time. The use of detachable windows enabled us to place the D_2O-soaked switchgrass particles in the cell so as to fill the entire beam spot homogeneously. Three different instrument configurations were employed to collect data over the range of scattering vectors $0.001 < Q < 0.3$ Å^{-1}, employing sample-to-detector distances of 1.2 and 6.9 m, both with a neutron wavelength (λ) of 6 Å, and 15.4 m with a neutron wavelength of 18 Å. $Q = (4\pi/\lambda)\sin\theta$ and 2θ is the scattering angle. In each case, the center of the area detector (Ordela 2410N) was offset by 150 mm from the beam. The instrument resolution was defined using circular aperture diameters of 40 mm for the source and 8 mm for the sample, which were separated by distances of 3.3 m for $0.03 < Q < 0.3$ Å^{-1}, 9.3 m for $0.0065 < Q < 0.06$ Å^{-1} and 17.4 m for $0.001 < Q < 0.009$ Å^{-1}. The relative wavelength spread was set to 0.15. The scattering-intensity profiles $I(Q)$ *versus* Q were obtained by azimuthally averaging the processed two-dimensional images, which were normalized to incident-beam monitor counts and corrected for detector dark current, pixel sensitivity and solvent-scattering backgrounds from D_2O and the quartz cell. The procedure used for proper solvent-background subtraction is as follows. The weight of the cell with the D_2O-soaked slurry sample was

measured before and after the experiment. The dry cell weight and vacuum-dried lignocellulose sample weights were also measured to obtain volume fractions of the solvent background to the solid sample. The solvent-background data were scaled to this ratio prior to subtraction.

SANS data were analyzed using the multi-level unified equation implemented in the *Irena* package (Ilavsky & Jemian, 2009) to elucidate the multiple levels of structural organization. For each individual level, i, the scattering signal is the sum of Guinier's exponential form and the structurally limited power law (Beaucage, 1995, 1996; Belina *et al.*, 2003),

$$I(Q) = \sum_{i=1}^{n}\left(G_i \exp\left(\frac{-Q^2 R_{g_i}^2}{3}\right) + B_i \exp\left[\frac{-Q^2 R_{g_{(i+1)}}^2}{3}\right]\left\{\frac{[\mathrm{erf}(QR_{g_i}/6^{1/2})]^3}{Q}\right\}^{P_i}\right) + I_{\mathrm{bkg}}, \quad (1)$$

where $i = 1, \ldots, n$. To model the lignocellulose SANS data, we used a total of three levels, with $i = 1$ and $i = 3$ referring to the smallest size and largest size structural levels, respectively. $G_i = c_i V_i \Delta\rho_i^2$ is the exponential prefactor, R_{g_i} is the radius of gyration of the ith kind of particle, B_i is a Q-independent prefactor specific to the type of power-law scattering with power-law exponent P_i and I_{bkg} is the flat background intensity arising from incoherent scattering. c_i is the concentration of the ith kind of particle, V_i is the volume of the ith kind of particle and $\Delta\rho_i$ is the contrast of the ith kind of particle with respect to the solvent. The expression of the constant prefactor is $B_i = (G_i P_i / R_g^{P_i})\Gamma(P_i/2)$ when the ith level is a mass fractal composed of elementary units of the next lowest [$(i-1)$th] level (Beaucage, 1996).

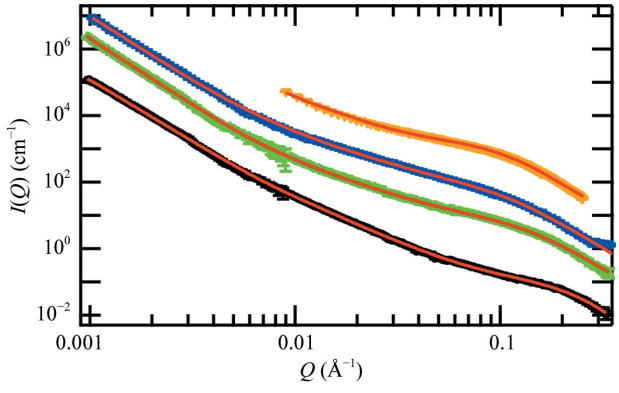

Figure 1
SANS data for native switchgrass (black), cellulose isolated from native switchgrass (green), cellulose isolated from dilute acid pretreated switchgrass (blue) and microcrystalline cellulose (Avicel; orange). The unified-fit model is shown in red solid lines. Extracted switchgrass cellulose and dilute acid pretreated switchgrass cellulose curves were scaled by factors of 10 and 100, respectively, from the unscaled native switchgrass curve. However, the Avicel data are plotted in arbitrary intensity units since originally they were not collected on an absolute scale.

Table 1
Comparison of SANS fit results and literature-reported values.

Q range (Å)	0.3–0.06	0.06–0.006	0.01–0.0001
Samples/fit parameters	R_g (Å)	P	P
Avicel PH-105	18.5 ± 0.5	—	—
Native switchgrass	8.7 ± 0.6	2.48 ± 0.09	3.94 ± 0.04
Cellulose isolated from			
Native switchgrass	13.6 ± 1.0	2.03 ± 0.09	3.99 ± 0.04
Dilute acid pretreated switchgrass	15.8 ± 1.5	1.82 ± 0.02	3.95 ± 0.04
High-Q fibril model interpretation			
Picea abies (Jakob *et al.*, 1996)	12.5 ± 0.7 (R)	—	—
Picea abies (Jakob *et al.*, 1995)	12.4 ± 0.2 (R)	—	—
High-Q pore model interpretation			
Fabriano perusia (sample F6; Missori *et al.*, 2006)	16.1 ± 0.4	1.8 ± 0.1	3.8 ± 0.2
Fabriano perusia (sample F6; De Spirito *et al.*, 2008)	15.1 ± 0.6	1.68 ± 0.04	3.7 ± 0.1
Avicel (FD100; Kent *et al.*, 2009)	17.0	1.4	3.5

3. Results

3.1. Extracted switchgrass cellulose

The SANS scattering curves of the native switchgrass material and the cellulose extracted from it are shown in Fig. 1 with their unified fits (Beaucage, 1995, 1996; Belina *et al.*, 2003). Based on changes in the curve features, the data may be divided into three distinct structural regimes of small ($Q > 0.06$ Å^{-1}), intermediate ($0.006 < Q < 0.06$ Å^{-1}) and large ($0.001 < Q < 0.006$ Å^{-1}) length scales. The corresponding length scales in real space are less than 100 Å, between 100 and 1000 Å and 1000–6000 Å, respectively. Each of the three structural regimes was fitted to a single level of the unified model (Beaucage, 1995, 1996; Belina *et al.*, 2003) in (1). The fit results for the different levels are summarized in Table 1. The radii of gyration, R_g, describing short length scales, obtained by fitting the data at large Q for native biomass and extracted cellulose are 8.7 ± 0.6 and 13.6 ± 1.0 Å, respectively. In the intermediate length-scale regime power-law behaviour is observed, with a change in the exponent from $P = 2.48 \pm 0.09$ for untreated switchgrass to 2.03 ± 0.09 for the extracted cellulose. A mass fractal dimension d_f of ∼2.5 ($d_f = P$) describes a randomly branched chain that follows a Gaussian path (Beaucage, 2004). This change in power-law behaviour is consistent with a decrease in the degree of branching when cellulose is isolated from the parent switchgrass material, which in this case can be interpreted as a decrease in the interconnectivity of the biopolymer network. Power-law scattering is observed at large length scales with exponents $P = 3.94 \pm 0.04$ and 3.99 ± 0.04, respectively. A power-law exponent close to 4.0 suggests surface scattering by smooth interfaces. For these samples, the implication is that the microscopic interfacial features of the extracted cellulose samples are not perturbed by processing, although the data do not cover all of the necessary length scales required to draw this conclusion unambiguously.

3.2. Dilute acid pretreated switchgrass cellulose

The SANS scattering curve of the cellulose extracted from dilute acid pretreated switchgrass is also shown in Fig. 1. The

unified-fit results are summarized in Table 1. This SANS curve has a Guinier regime at small length scales ($Q > 0.06$ Å^{-1}), similar to native switchgrass and the cellulose extracted from it. The radius of gyration R_g is 15.8 ± 1.5 Å and is significantly larger than those found for native switchgrass or the cellulose extracted from native switchgrass. The observed power-law scattering exponent, $P = 1.82 \pm 0.02$, is close to the value observed for extracted cellulose without pretreatment and clearly differs from that of the intact native switchgrass sample. The nature of the change in the material network is not clear from this slope, but it suggests that the network is more open than in the cellulose extracted from native switchgrass. At large length scales ($0.001 < Q < 0.006$ Å^{-1}) the extracted cellulose from pretreated switchgrass shows a power-law scattering profile with an exponent of $P = 3.95 \pm 0.04$, again suggesting smooth surfaces and that little about the microscopic surface structure of the material changes in response to pretreatment.

3.3. Microcrystalline cellulose: Avicel

The SANS scattering profile of Avicel was measured in the range $0.01 < Q < 0.3$ Å^{-1} (Fig. 1) for comparison with that of switchgrass cellulose. Analysis of the Avicel data clearly shows a Guinier-type profile at high Q, similar to the feature seen in the celluloses extracted from native and dilute acid pretreated switchgrass. The location of the bend in the curve is at a smaller Q than for all other samples discussed above and the extracted R_g of 18.5 ± 0.5 is correspondingly larger, implying that the processing that produces highly crystalline Avicel, *i.e.* dilute hydrochloric acid treatment to remove amorphous cellulose and formation of colloidal dispersions by high-shear fields, followed by spray-drying of the washed slurry, further drives the growth of the well defined relatively small structures within the material.

4. Discussion

Dilute acid pretreatment is a standard industrial protocol that has been optimized to maximize the enzymatic conversion of cellulose to sugars while minimizing cost through a one-boiler-step approach using dilute aqueous sulfuric acid. On the other hand, the multiple-step method used to isolate cellulose from native switchgrass, as described in §2.1, is designed to extract cellulose from biomass while minimizing the changes to the cellulose structure in order to obtain material for analysis by NMR and other methods. As expected, the structural features of isolated cellulose differ considerably from those of native switchgrass. Furthermore, the structural features of cellulose isolated from native and acid pretreated switchgrass also differ. The main structural differences observed are in the Q range $0.3 < Q < 0.006$ Å^{-1}: a decrease in the power-law exponent from 2.48 to ∼2 (or 1.82) and an increase in the radius of gyration in the high-Q region from 8.7 to 13.6 Å (or 15.8 Å).

A decrease in the power-law exponent indicates a reduction in the degree of branching (Beaucage, 2004), which is related to a reduction in the interconnectivity of the fibrils and/or removal of the branched amorphous biopolymers hemicellulose and lignin. The small difference in the power-law exponent between isolated cellulose samples from native (2.03) and pretreated switchgrass (1.82) arises owing to a greater breakdown of the cellulose fibril network structure at length scale of 100–200 Å by dilute acid pretreatment.

SANS detects scattering contrast between phases with different scattering-length density and for the present system two alternate pictures may be proposed: crystalline cellulose fibrils in a sea of solvent-soaked amorphous biomass (fibril model) or solvent pores in a matrix of continuous biomass (pore model) (Kent *et al.*, 2009). Table 1 includes reported literature results for different sources of cellulose interpreted using either of the two alternate contrast models. The high-Q roll-off ($Q > 0.06$ Å^{-1}) or R_g values for all switchgrass and literature-reported samples of both fibril and pore models are in the range 10–20 Å. The cross-sectional R_g value of the elementary cellulose fibril (ECF), which consists of 36 cellulose chains, has been estimated to be ∼9 Å or equivalently a radius of 12.5 Å as listed in Table 1 (Jakob *et al.*, 1995, 1996) and 8–15 Å (Ding & Himmel, 2006) depending on the extent of the crystalline core of the ECF. The R_g values for native switchgrass and for cellulose isolated from native and dilute acid pretreated switchgrass fall within the literature-reported values of the R_g of the ECF. An increase in R_g for the cellulose isolated from switchgrass compared with the native switchgrass sample indicates an increase in the radius of the crystalline core of the ECF. This increase in the crystalline core of the ECF may be promoted by the removal of the amorphous biopolymers hemicellulose and lignin from the periphery of the ECF and the high temperature, which functions as an annealing process for the crystallization of cellulose strands.

Although an increase in ECF crystallinity is understood to be counterproductive in increasing the efficiency of cellulose-hydrolysis, the processes of hemicellulose removal and lignin redistribution could play a dominant role in increasing the cellulose-hydrolysis efficiency. Recently, Chung and coworkers reported a fivefold increase using straight saccharification from 18.0 ± 4.1% cellulose conversion for native switchgrass to 91.4 ± 3% cellulose conversion for dilute acid pretreated switchgrass (1.5% acid at 453 K for 0.5 min; Chung *et al.*, 2005).

5. Conclusions

We have used SANS to probe the structures of cellulose samples extracted from switchgrass across multiple length scales. Cellulose preparations from native and dilute acid pretreated switchgrass were compared with microcrystalline cellulose (Avicel) and with the scattering signature of intact native switchgrass. The results demonstrate a considerable structural alteration of the material at length scales of 10–1000 Å, but little impact on the longest length scales studied (1000–6000 Å). The characteristic dimension R_g at high Q of microcrystalline cellulose (Avicel) closely agrees with that of cellulose extracted from pretreated switchgrass, but is almost

double the value obtained for the native switchgrass material. The cellulose sample from the cellulose-isolation process using native switchgrass also exhibits an increase in the small-scale structure R_g compared with the untreated native material, although the effect is less pronounced. In addition, comparison of cellulose extracted from both pretreated and native switchgrass with native switchgrass shows a reduction in the network interconnectivity from a highly branched or folded structure to a less branched or folded structure, as indicated by a change in the power-law exponent in the intermediate-Q regime. Interestingly, neither the cellulose-extraction process nor dilute acid pretreatment have a significant effect on the large-scale structure at length scales greater than 1000 Å, which in all cases is best described as scattering from nearly smooth surfaces. Interestingly, the high-Q characteristic dimensions of the extracted cellulose from pretreated and native switchgrass closely resemble the reported literature values for the elementary cellulose fibril radius (Ding & Himmel, 2006; Jakob *et al.*, 1995, 1996) and therefore the observed change may be related to an increase in the cellulose fibril radius of the processed switchgrass cellulose relative to the native material. However, such an increase would appear to be counterproductive to achieving improved enzymatic digestibility of cellulose. On the other hand, dilute acid pretreatment is known to redistribute lignin (Woerner & McCarthy, 1988; Vainio *et al.*, 2004; Donohoe *et al.*, 2008) as well as to dissolve hemicellulose (Foston & Ragauskas, 2010). We therefore propose that the latter effects are the primary reason for the efficacy of dilute acid pretreatment, while changes in the cellulose morphology and structure are of less importance and may even be counterproductive to the goal of increasing digestibility through pretreatment.

Switchgrass samples were obtained through a collaborative agreement with the Bioenergy Science Center (BESC) located at the Oak Ridge National Laboratory, Oak Ridge, Tennessee. This research is funded by the Genomic Science Program, Office of Biological and Environmental Research, US Department of Energy, under FWP ERKP752. Initial studies on Avicel were funded by the ORNL Laboratory Directed Research and Development Seed Money Fund under project No. S07-019. This research at Oak Ridge National Laboratory's Center for Structural Molecular Biology (CSMB) was supported by the Office of Biological and Environmental Research, using facilities supported by the US Department of Energy, managed by UT-Battelle LLC under contract No. DE-AC05-00OR22725.

References

Beaucage, G. (1995). *J. Appl. Cryst.* **28**, 717–728.
Beaucage, G. (1996). *J. Appl. Cryst.* **29**, 134–146.
Beaucage, G. (2004). *Phys. Rev. E*, **70**, 031401.
Belina, G., Urban, V., Straube, E., Pyckhout-Hintzen, W., Kluppel, M. & Heinrich, G. (2003). *Macromol. Symp.* **200**, 121–128.
Bouton, J. (2008). *Genetic Improvement of Bioenergy Crops*, edited by W. Vermerris, pp. 295–308. New York: Springer.
Bouton, J. H. (2007). *Curr. Opin. Genet. Dev.* **17**, 553–558.
Chung, Y.-C., Bakalinsky, A. & Penner, M. (2005). *Appl. Biochem. Biotechnol.* **124**, 947–961.
De Spirito, M., Missori, M., Papi, M., Maulucci, G., Teixeira, J., Castellano, C. & Arcovito, G. (2008). *Phys. Rev. E*, **77**, 041801.
Ding, S.-Y. & Himmel, M. E. (2006). *J. Agric. Food Chem.* **54**, 597–606.
Donohoe, B. S., Decker, S. R., Tucker, M. P., Himmel, M. E. & Vinzant, T. B. (2008). *Biotechnol. Bioeng.* **101**, 913–925.
Esteghlalian, A., Hashimoto, A. G., Fenske, J. J. & Penner, M. H. (1997). *Bioresour. Technol.* **59**, 129–136.
Foston, M., Hubbell, C., Davis, M. & Ragauskas, A. (2009). *Bioenergy Res.* **2**, 193–197.
Foston, M. B. & Ragauskas, A. J. (2010). Submitted.
Himmel, M. E., Ding, S.-Y., Johnson, D. K., Adney, W. S., Nimlos, M. R., Brady, J. W. & Foust, T. D. (2007). *Science*, **315**, 804–807.
Ilavsky, J. & Jemian, P. R. (2009). *J. Appl. Cryst.* **42**, 347–353.
Jakob, H. F., Fengel, D., Tschegg, S. E. & Fratzl, P. (1995). *Macromolecules*, **28**, 8782–8787.
Jakob, H. F., Tschegg, S. E. & Fratzl, P. (1996). *Macromolecules*, **29**, 8435–8440.
Kent, M. S. *et al.* (2009). *Biomacromolecules*, **11**, 357–368.
Lee, I., Evans, B. R. & Woodward, J. (2000). *Ultramicroscopy*, **82**, 213–221.
Lynd, L. R., Cushman, J. H., Nichols, R. J. & Wyman, C. E. (1991). *Science*, **251**, 1318–1323.
Lynn, G. W., Heller, W., Urban, V., Wignall, G. D., Weiss, K. & Myles, D. A. A. (2006). *Physica B*, **385–386**, 880–882.
McMillan, J. D. (1994). *Enzymatic Conversion of Biomass for Fuels Production*, edited by M. E. Himmel, J. O. Baker & R. P. Overend, pp. 292–324. Washington DC: American Chemical Society.
Missori, M., Mondelli, C., De Spirito, M., Castellano, C., Bicchieri, M., Schweins, R., Arcovito, G., Papi, M. & Castellano, A. C. (2006). *Phys. Rev. Lett.* **97**, 238001.
Schell, D., Farmer, J., Newman, M. & McMillan, J. (2003). *Appl. Biochem. Biotechnol.* **105**, 69–85.
Vainio, U., Maximova, N., Hortling, B., Laine, J., Stenius, P., Simola, L. K., Gravitis, J. & Serimaa, R. (2004). *Langmuir*, **20**, 9736–9744.
Woerner, D. L. & McCarthy, J. L. (1988). *Macromolecules*, **21**, 2160–2166.
Zhang, Y.-H. P., Himmel, M. E. & Mielenz, J. R. (2006). *Biotechnol. Adv.* **24**, 452–481.
Zhang, Y.-H. P. & Lynd, L. R. (2004). *Biotechnol. Bioeng.* **88**, 797–824.